

Flow angle dependence for the asymmetry of broad 50-MHz coherent echoes at large magnetic aspect angles

A. V. Kustov¹, G. J. Sofko¹, J. A. Koehler¹, M. V. Uspensky²

¹Institute of Space and Atmospheric Studies, University of Saskatchewan, 116 Science Place, Saskatoon, Saskatchewan, S7N 5E2, Canada

²Murmansk State Technical University, Murmansk, Sportivnaya, 1, 183023 Russia

Received: 27 November 1996 / Revised: 10 February 1997 / Accepted: 27 February 1997

Abstract. The skewness of broad Type 2-like spectra has been studied using data collected by two orthogonal CW 50-MHz radio links with co-located scattering volumes. Geometrical aspect angles of observations were about 10° . One short event was considered. For this event, the electron flow direction was changing periodically (period about 9 minutes) presumably due to the passage of a magnetospheric MHD wave through the ionosphere. It was found that for the radar observations along the electrojet flow, the skewness had the same sign as the mean Doppler shift with average absolute values in between 0.5–1.0. For observations perpendicular to the electrojet flow, spectra were more symmetrical (average skewness was around 0) and the sign of the skewness was sometimes opposite to the sign of the mean Doppler shift. These observations are interpreted in terms of contribution from both the Farley-Buneman and gradient-drift instabilities to the resultant spectrum. Differences with radar observations at small aspect angles are discussed.

1 Introduction

Recent 50-MHz radar observations in the Canadian Arctic showed that, even at very unfavourable geometrical aspect angles of more than 10° , echoes occurred at least 5% of the observational time (Kustov *et al.*, 1994; 1995). For these large aspect echoes, as for those observed at small aspect angles of several degrees, all known types of spectra have been identified (Haldoupis, 1989; Osterried, 1993).

Of all the echoes observed, those with broad spectra were longer in duration than other types of spectra, especially for large magnetic disturbances of more than 400–500 nT (Osterried, 1993). These echoes varied

slowly in time and space and persisted for several hours. Typically, broad spectra were observed simultaneously at different flow angles, similar to small aspect type 2 echoes during low ambient electric field conditions, when the gradient-drift instability is the likely source of irregularities. This was the reason why the large aspect angle broad spectra were labelled type 2 (Kustov *et al.*, 1994). What distinguished these echoes from classical type 2 echoes was their mean Doppler shift; sometimes these echoes had a mean Doppler shift in excess of the ion-acoustic velocity.

For background plasma flow faster than the ion-acoustic velocity, the Farley-Buneman instability is another source of metre-scale irregularities. At small aspect angles, the Farley-Buneman instability can generate narrow type 1 irregularities which results in a strong power increase along the electrojet direction. At large aspect angles, however, echoes along the electrojet (parallel echoes) were usually not narrow type 1-like but broad, type 2-like, even for electric fields as large as 60 mV/m (Kustov *et al.*, 1997). The intensity of these broad parallel echoes was about the same as that of echoes simultaneously observed perpendicular to the electrojet (perpendicular echoes). The spectral width of the parallel echoes was even slightly greater than that for the perpendicular echoes (Kustov *et al.*, 1995). These observations suggest that the effect of the Farley-Buneman turbulence at large aspect angles is sometimes not as pronounced as it is at small aspect angles. One should mention that narrow type 1-like echoes were also observed at large aspect angles, but not as regularly as at small aspect angles (Osterried, 1993). Kustov *et al.* (1997) suggested that these narrow type 1/type 3 echoes occur when radar waves experience strong ionospheric refraction so that small aspect angles are achieved, as was predicted by Uspensky and Williams (1988) and Uspensky *et al.* (1994).

Kustov *et al.* (1994) and Osterried *et al.* (1995) studied the shape of large aspect angle broad type 2 echoes. The shape of spectra was characterized by the third moment in the power spectral distribution, the

skewness. For an asymmetric spectrum with a tail towards higher (smaller) frequencies in a spectral power distribution, skewness is positive (negative). It was discovered that large aspect angle and small aspect angle broad echoes are typically skewed differently. At large aspect angles, spectra with a positive mean Doppler shift have positive skewness and spectra with a negative mean Doppler shift have negative skewness. The situation is opposite for small aspect angles; positive skewness occurs with negative mean Doppler shift and negative skewness with positive mean Doppler shift.

Osterried *et al.* (1995) hypothesized that this difference was, at least partially, due to variation in the ratio of the Farley-Buneman turbulence to the gradient-drift turbulence contributions into resultant broad spectra. At small aspect angles, a broad type 2 spectrum is a superposition of scattering from weak gradient-drift waves, distributed isotropically in all flow directions, and strong Farley-Buneman waves dominating in the wide cone of flow angles along the electrojet direction. This explanation was given first by Greenwald *et al.* (1975) and later confirmed in several studies (e.g., Haldoupis *et al.*, 1984). At large aspect angles, according to Osterried *et al.* (1995), the contribution from the Farley-Buneman waves to the resultant spectrum is not so great in power, and the Farley-Buneman spectral line itself is rather broad. In this case, skewness of the spectrum could be positive for positive mean Doppler shift. No other reasonable explanations for difference in skewness of small and large aspect type 2 echoes have been offered. One should mention that current theories of the Farley-Buneman and gradient-drift turbulence explain only the small aspect angle results (see discussion in Osterried *et al.*, 1995).

Though Osterried *et al.* (1995) stated that the signs of skewness and mean Doppler shift were the same, there were numerous spectra for which the signs of skewness and mean shift were actually different, unlike those for the bulk of echoes (see their Fig. 6). Moreover, Kustov *et al.* (1994) found a similarity in skewness between broad type 2 spectra observed in the polar cap and the small aspect angle ones. These facts might cast a doubt in conclusion of Osterried *et al.* (1995). However, more recent radar observations of Kustov *et al.* (1996) using the SAPPHERE-North radar showed that for observations perpendicular to the electrojet, the spectra could be skewed both positively and negatively for positive mean Doppler shift. Only for observations along the electrojet is there agreement in the signs of skewness and mean Doppler shift. This conclusion cannot be substantiated (or rejected) with Osterried *et al.*'s (1995) data; typical flow angles of those observations were 40–50 degrees for both radio links and there were very few events with velocities in excess of 300–400 m/s, for which the effect of the Farley-Buneman turbulence could be strong.

In this study, data of the same auroral zone radar experiment that was used by Osterried *et al.* (1995), are considered for one unique event, April 04, 1993. During this event, strong quasi-periodic variations of the electrojet flow direction occurred, so that the hypothesis of Osterried *et al.* (1995) regarding the relationship of

skewness of type 2 spectra and the flow angle of radar observations could be checked in a straightforward manner.

2 Experiment

On April 04, 1993 two CW 50-MHz radio links with nearly overlapping scattering volumes were operational in the Canadian Prairies as shown in Fig. 1. Transmitters were located at LaCrete (Alberta) and Gillam (Manitoba), and the receiver was in Saskatoon (Saskatchewan). The antenna arrays for both transmitter sites were 8 Yagis separated by 6 m. The receiving antenna was polarimetric; it consisted of two sets of 12 Yagis oriented at the angles 45° and 135° with respect to the horizon. The main collecting regions for both links were about 50 × 50 km² (at the 6-dB level of attenuation) in size so that there was a partial overlapping of these regions.

The experiment was run in a mode with the reception of scattered signals on both 45° and 135° polarimetry antennae but, as was discovered later, the 135° channel had technical problems so that data from that channel were not used for this study. To smooth the temporal variations of signals, 10-s averaging of the spectra was applied. More detailed description of the radio links can be found elsewhere (Kustov *et al.* 1995; Osterried *et al.*, 1995).

3 Observations

On April 4, 1993, the CANOPUS Rabbit Lake magnetometer (for CANOPUS see Grant and McDiarmid, 1992) located near the radar target regions showed that the magnetic field was quite stable almost the whole night except for small and smooth magnetic variations around local magnetic midnight. This was typical across

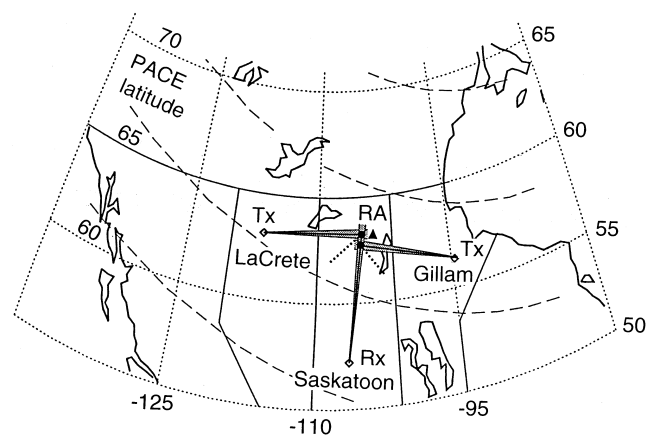


Fig. 1. The geometry of the experiment. Two transmitters were located at LaCrete and Gillam, two receivers at Saskatoon. Invariant latitudes according to the Polar Anglo-American Conjugate Experiment (PACE) coordinate system (Baker and Wing, 1989) are shown by dashed lines. The link bisectors are marked by thick dotted line. Black triangle is the location of Rabbit Lake (RA) magnetometer site

the entire world; Kp indices were between 1 and 2 (Coffey, 1993). Figure 2 shows a standard Rabbit Lake magnetogram. A very strong and sharp onset of magnetic activity occurred at about 1500 UT (about 0900 MLT). This magnetic activity started with a strong SC (sudden commencement) impulse at 1432 UT recorded not only in Rabbit Lake but in many other places around the world, e.g. according to European SAMNET magnetometer records (M. Lester, private communication, 1993). About 20 minutes later, the magnetic field X-component in Rabbit Lake began a rapid negative trend reaching magnitudes of -800 nT after 1500 UT. Simultaneously strong variations in Y and Z components of several hundred nanoteslas were observed (see, for example, in Fig. 2 variations in the Y-component). After 1800 UT, a quick recovery of the magnetic field occurred.

The sharp onset of magnetic variations at 1450 UT was followed by strong temporal fluctuations of the magnetic field at Pc5 range (period of ~ 9 minutes according to FFT analysis), see Fig. 2. These oscillations were particularly pronounced in the Y-component of the magnetic field. Strong magnetic pulsations lasted till about 1630 UT.

These strong periodic variations in the magnetic field were accompanied by periodic broad type 2 echoes on both the G-S and L-S radio links. Strong variations in echo parameters were evident during the first hour of echo onset though the echoes lasted until about 1800 UT, as shown by the horizontal bar in the middle panel of Fig. 2. Clearly, echoes occurred for magnetic disturbances of more than 400–500 nT, in agreement with Osterried (1993).

Figure 3 shows the spectral distribution of the G-S link power versus time for the period 1500–1600 UT, for which the radar pulsations were very clear. Variations in the width of the echoes can also be recognized. Similar echo pulsations, but not as clear as these, were observed on the L-S link.

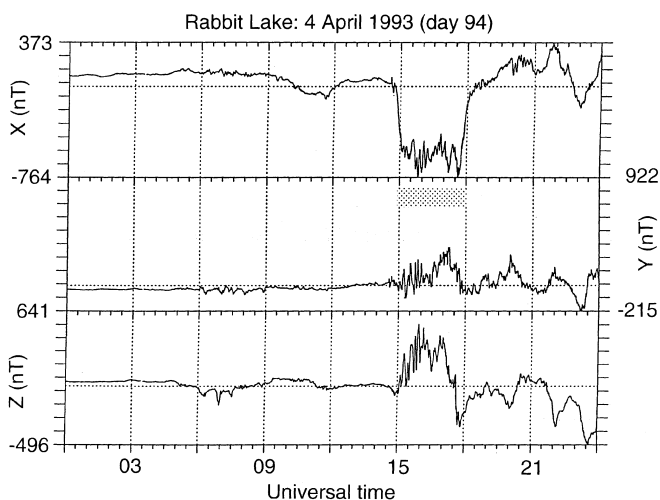


Fig. 2. Magnetic variations recorded at Rabbit Lake on April 4, 1993. The horizontal bar on the middle panel indicates the times of 50-MHz coherent echo occurrence

Figure 4 shows temporal behaviour of the power (a), mean Doppler velocity (b) and skewness (c) of the spectra for both radio links during the first hour of the radar auroral activity. The L-S link data are shown by a thick line and the G-S link data are shown by a thin line. Pulsations in power (Fig. 4a) were more obvious for the G-S link where differences between the minimum and maximum power were as large as 7 dB. The echo intensity on both links was low with mean values of 5–10 dB (note that direct comparison of the power between two links is inappropriate since radio links were not properly calibrated).

Velocity pulsations (Fig. 4b), especially for the G-S link, were very clear. The magnitude of the variations was about 400 m/s for the G-S link and 300 m/s for the L-S link. It is obvious that the velocity changes for the L-S link were roughly in phase with the velocity changes for the G-S link (with some DC offset); large positive values of the G-S velocity occurred at times of minimal negative velocity on the L-S link and vice versa. This effect is illustrated in Fig. 4 for two specific times labelled 1 and 2.

The observed velocity variations can be interpreted as a result of periodic variations in the electron flow azimuth. Since the mean Doppler velocity of the broad type 2 echoes is proportional to the cosine component of the plasma flow along the radar link bisector (Kustov *et al.*, 1997), the electron flow azimuth can be determined by simply merging the L-S and G-S mean Doppler velocities (see Nielsen and Schlegel, 1985). Figure 4c shows temporal variations of the electron flow azimuth θ during the interval under consideration. Note that the azimuth is measured CCW from the east (rather than normally the north). Clearly, the flow azimuth varied periodically between two extremes, $\theta_1 = -40^\circ$ and $\theta_2 = +50^\circ$. The first extreme corresponds to electron flow along the G-S radio link bisector (as at the time labelled 1) while the second extreme corresponds to the electron flow almost along the L-S radio link bisector (as at the time labelled 2).

Variations of the electron flow direction shown in Fig. 4c are the superposition of a background flow directed eastward along the lines of constant PACE latitude (the mean electron flow azimuth in Fig. 4c is around zero) and a periodic north-south flow. A clear possibility is that the periodic north-south component of the flow is associated with a MHD wave which has propagated down the Earth's magnetic field lines into the radar scattering volume (Yeoman *et al.*, 1990). This suggestion is supported by the Rabbit Lake magnetometer data. In Fig. 4, the Y-component of the magnetic field (which has been pass-filtered for periods between 250 and 1000 s) is shown. Vertical bars indicate the times when the electron flow is along the G-S radio link ($\theta_1 = -40^\circ$), which should be the times when the Y-component has maximum negative deviations. Good agreement of these bars and the magnetometer trace minima is obvious for almost the whole period of observations.

Also obvious from Fig. 4 is that the relationship between the power and velocity was different for the L-S

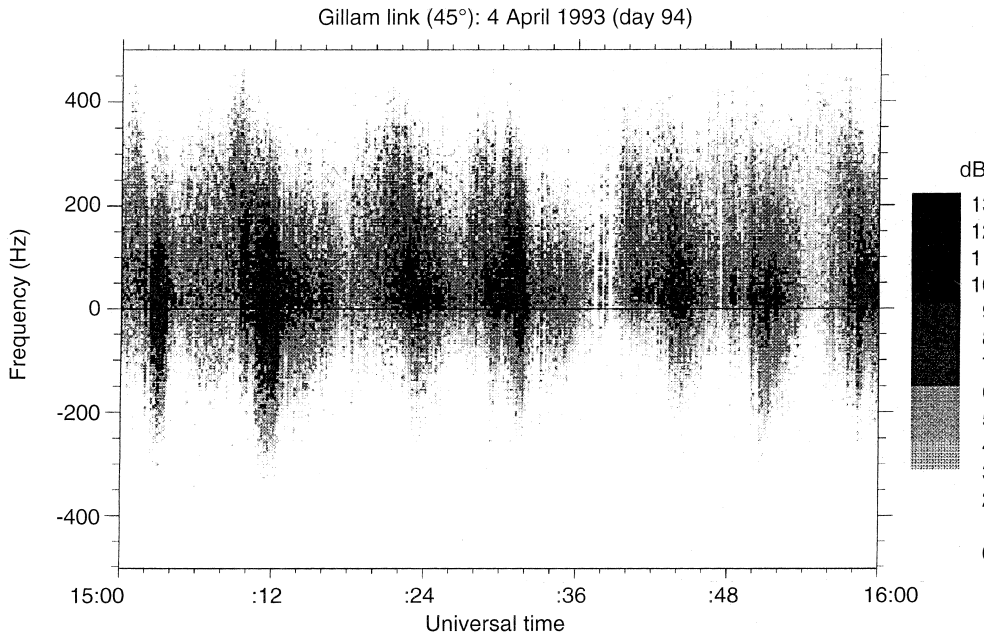


Fig. 3. Doppler spectra of coherent echoes received on April 4, 1993 on the Gillam-Saskatoon 50-MHz radio link. To obtain the mean velocity shift and spectral width the values in Hz should be multiplied by a factor 3.1

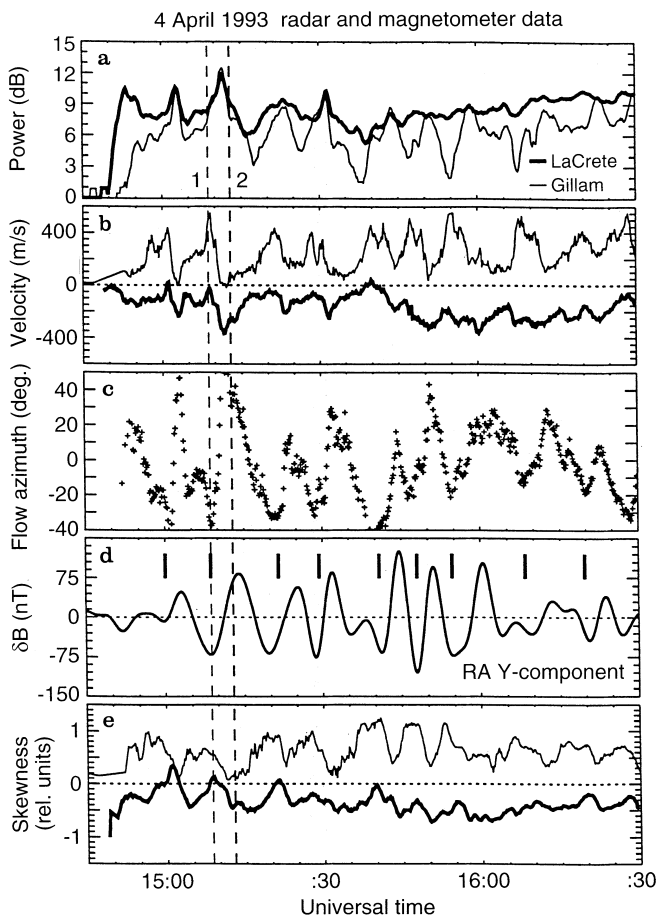


Fig. 4a-e. Temporal behaviour of the power **a**, mean Doppler velocity **b** and skewness **e** on the Gillam-Saskatoon (*thin line*) and LaCrete-Saskatoon (*thick line*) radio links during the period of pulsations. **c** Shows flow azimuth (CCW from the east) inferred from the G-S and L-S Doppler velocities. **d** Shows the rectified Y-component (east-west) of the Rabbit Lake magnetogram

and G-S links. For the L-S link, the power and velocity varied in phase. One can see a nearly simultaneous occurrence of peaks in the velocity and power at 1502, 1511, 1524 and 1531 UT (later on, the L-S echo power pulsations disappeared). For the G-S link, the power and the velocity were not in phase, the velocity maxima were somewhere in between the power maxima and minima (see times of 1501, 1509, 1521, 1529 and so on). Comparison with riometer recordings at Rabbit Lake showed that the echo power on both links correlated with intensifications of absorption. This suggests that the echo power was strongly influenced by conductivity variations rather than electric field variations. Similar results have been obtained by Yeoman *et al.* (1990) for higher frequency radar and magnetic pulsations.

In Fig. 4e, the skewness versus time is plotted for both links. Pulsations with a period of about 9 min are also seen. Moreover, the maxima of G-S skewness correlate well with the minima of the absolute value of L-S skewness. The maxima of G-S skewness correspond to the G-S velocity maxima. Such a relationship is not obvious for the L-S spectra, in agreement with results of Osterried *et al.* (1995). The relationship between skewness and velocity of spectra is evaluated quantitatively in the next two sections.

4 Skewness versus radial velocity

In Fig. 5 the relationship between signs of the mean Doppler shift and skewness is explored in a way similar to Osterried *et al.* (1995). First, only those measurements were considered for which G-S velocities were larger (in absolute value) than L-S velocities (Fig. 5a). This would imply that the G-S radio link bisector was closer to the electrojet direction than the L-S radio-link bisector. Skewness of the spectra on the L-S link (S_L) versus skewness of the spectra on the G-S link (S_G) is presented

4 April 1993 (day 94: 14:45-16:30 UT)

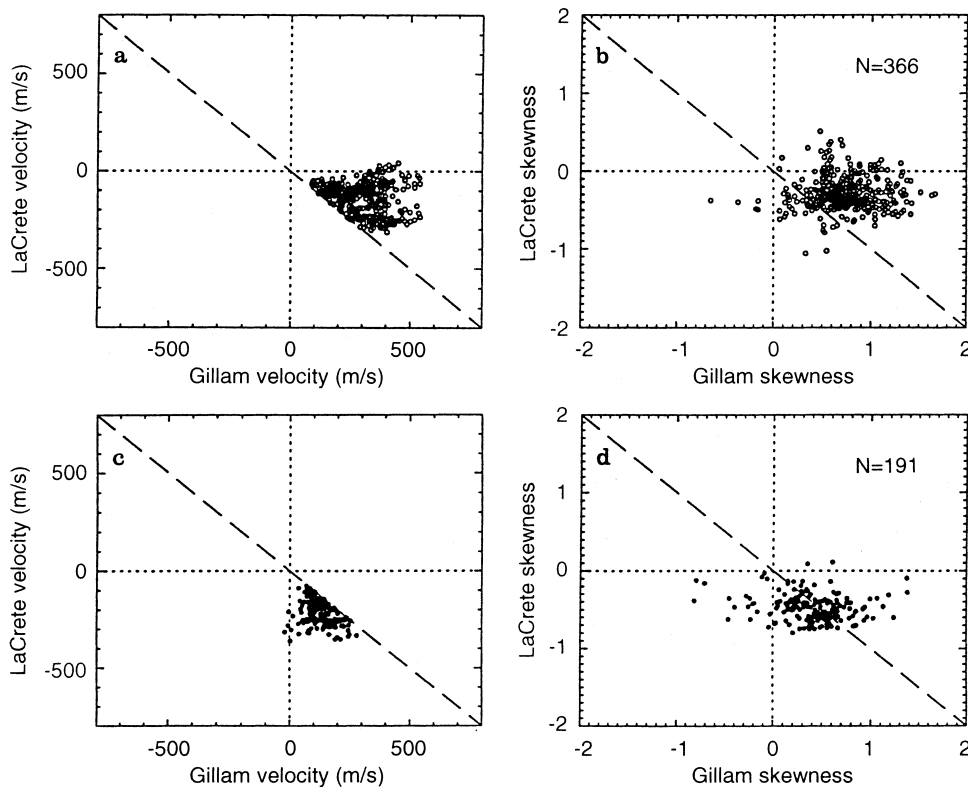


Fig. 5a–d. Scatterplot of skewness at the LaCrete-Saskatoon link versus skewness at the Gillam-Saskatoon link: **b** For the cases when the mean electron flow was closer to the Gillam-Saskatoon link bisector as shown in **a**; **d** For the cases when the mean electron flow was closer to the LaCrete-Saskatoon radio link as shown in **c**

in Fig. 5b. Clearly, $S_G > S_L$ for most of the measurements. Then, measurements with L-S velocities larger than G-S velocities (the L-S bisector closer to the electrojet direction) were considered (Fig. 5c). For these times, the cloud of points was definitively shifted towards stronger skewness on the L-S link, though not entirely (Fig. 5d).

5 Skewness versus flow angle

To describe the flow angle variation of the skewness in a more quantitative manner, measurements of the skewness for the G-S and L-S radio links were plotted in Fig. 6 as a function of the electron drift azimuth θ .

Figure 6a shows the scatter plot of the G-S skewness versus θ (points) and the statistical trend in this dependence (large circles). Each large circle in Fig. 6 was obtained by binning the skewness within 10° -bins in θ , beginning from $\theta = -40^\circ$. In each bin, the mean value (circle) and the standard deviation σ (vertical bar around each circle spans the range from $-\sigma$ to $+\sigma$) were calculated. From Fig. 6a, one can see that the G-S skewness decreases almost linearly from about $+1.0$ at $\theta_1 = -40^\circ$ (at which angle the flow is almost along this link bisector) to ≈ 0 at $\theta = +40^\circ$ (for which the flow is almost perpendicular to this link bisector). In Fig. 6b, the L-S skewness is plotted versus θ . These data demonstrate the linear increase of skewness, but one should keep in mind that, for the L-S radio-link, $\theta_1 = -40^\circ$ corresponds to observations almost perpen-

dicular to the electron flow and $\theta = +40^\circ$ corresponds to observations almost along the link bisector.

In Fig. 6c, the average trend in the dependence of the skewness versus θ for the G-S radio link is presented simultaneously with the trend in the absolute value of the L-S skewness. Obviously, when the electron flow was along the G-S radar link bisector ($\theta_1 = -40^\circ$), the G-S spectra were much more skewed while when the electron flow was along the L-S radio link bisector ($\theta = +40^\circ$), the L-S spectra were more skewed. Also, for observations along the electron flow, spectra were more skewed on the G-S radio link.

6 Discussion and conclusions

Observations of the asymmetry of auroral type 2 spectra reported in this study are in agreement with the majority of Osterried *et al.*'s (1995) measurements and support the conclusions of other observations performed with similar radio links but at higher latitudes (Kustov *et al.*, 1994; 1996). Along the electrojet direction, the skewness of the spectra is positive (negative) for positive (negative) mean Doppler shift while across the electrojet any combination of velocity and skewness sign is possible. In addition, this work shows that spectra are more asymmetric for observations along the electrojet.

Osterried *et al.* (1995) reviewed several ideas for explanation the unusual asymmetry of large aspect angle broad echoes observed along the electrojet. Their basic conclusion was that none of the current theories are

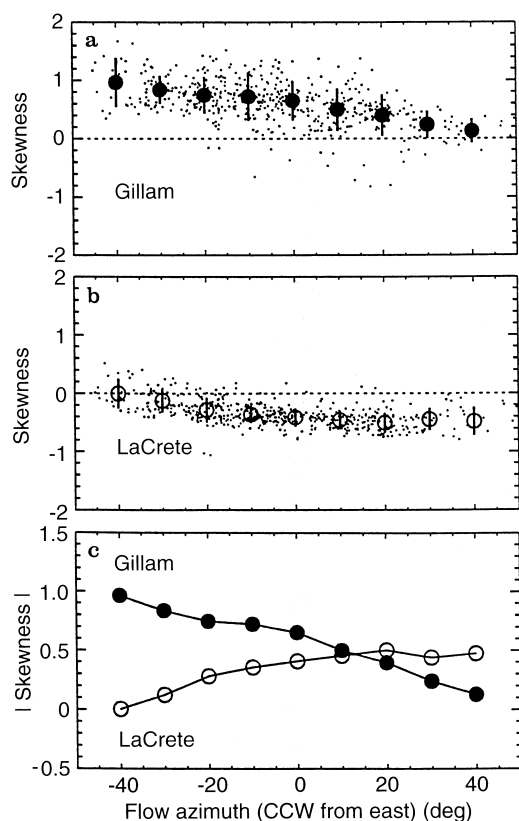


Fig. 6a–c. Dependence of the skewness versus the electron flow azimuth: **a** Scatterplot of skewness versus azimuth at the Gillam-Saskatoon link and the trend in this dependence (*large circles*); **b** the same as **a**, but for the LaCrete-Saskatoon link; **c** comparison of the trends on the G-S and L-S links

successful. The most likely reason for this difficulty lies in the fact that the echoes considered are indeed the large aspect angle ones. At the large aspect angles, plasma waves can be only generated nonlinearly by either the Farley-Buneman or the gradient-drift instability or both. The skewness of the resultant spectrum is strongly dependent on the relative contribution from each of these instabilities.

For low electric fields and for small aspect angles, when only the gradient-drift instability is operational, one might expect the symmetrical spectra as suggested in the mode-coupling theory (e.g., Sudan, 1983). A small asymmetry might arise from plasma turbulence itself, as known from simulations (Keskinen *et al.*, 1979, their Fig. 6). Another factor contributing to the measured asymmetry might be the effects of altitude integration (Kustov and Uspensky, 1995). All these effects cause negative skewness for positive Doppler shift. It is difficult to assess their importance at the large aspect angles relevant to the present study.

For stronger electric fields, the Farley-Buneman instability is operational, and it also contributes to the resultant spectrum. One would expect that the Farley-Buneman turbulence contribution is more important for observations along the electrojet, the direction for which the instability is much easier to excite. However, since the Farley-Buneman instability is excited directly only in

a relatively narrow cone of small aspect angles, its effect might not be very strong at large aspect angles. For large aspect angles, it might be that non-linearly excited (secondary) Farley-Buneman waves have a wider frequency band (not resonant peak at the ion-acoustic velocity as at small off-perpendicular angles) and they are distributed more isotropically with the flow angle. In this case, the spectrum along the electrojet would be composed of a symmetrical background gradient-drift/Farley-Buneman spectrum (as at any large flow angle) and an extra high frequency tail. More theoretical work is required to justify this hypothesis.

Interpreting the asymmetry of broad large aspect echoes as a flow angle effect in which the contribution from the Farley-Buneman instability is not very strong (as compared to the small aspect angle situation) implies that asymmetry of spectra should vary as the aspect angle increases. This idea is under investigation using 50-MHz SAPHIRE-South radar data (Koehler *et al.*, 1995). Preliminary analysis shows that, for some events, there is an increase in spectral asymmetry with aspect angle. This tendency is not obvious in others. More work is required to understand the reasons for different tendencies derived from the SAPHIRE-South data. In clarifying this issue, one of the problems is separating velocity variations due to aspect angle effect from those due to flow angle effect. Recent observations also show that, since the antenna arrays were tapered so that the side lobes were decreased, the spectra seem to be more symmetrical than in previous observations, which suggests that side lobe effects might be of importance.

Acknowledgements. Funding for this study has been provided by NSERC operating grants (to G.J.S. and J.A.K.) and Canadian Space Agency grant (to A.V.K.). Authors are thankful to R. Osterried and G. Hussey for running this experiment as a part of their thesis work. The magnetometer data were obtained through the Canadian Space Agency's CANOPUS project. The use of the facilities of the Institute of Space and Atmospheric Studies (University of Saskatchewan) is acknowledged.

Topical Editor D. Alcaydé thanks T. K. Yeoman and another referee for their help in evaluating this paper.

References

- Baker, K., and S. Wing, A new magnetic coordinate system for conjugate studies at high latitudes, *J. Geophys. Res.*, **94**, 9139–9143, 1989.
- Coffey, H., Geomagnetic and solar data, *J. Geophys. Res.*, **98**, 19,473–19,476, 1993.
- Grant, I. F., D. R. McDiarmid, and A. G. McNamara, A class of high-m pulsations and its auroral radar signature, *J. Geophys. Res.*, **97**, 8439–8451, 1992.
- Greenwald, R. A., W. L. Ecklund, and B. B. Balsley, Diffuse radar aurora: spectral observations of non-two-stream irregularities, *J. Geophys. Res.*, **80**, 131–139, 1975.
- Haldoupis, C., A review on radio studies of auroral E-region ionospheric irregularities, *Annales Geophysicae*, **7**, 239–258, 1989.
- Haldoupis, C., E. Nielsen, and H. M. Ierkić, STARE Doppler studies of westward electrojet radar aurora, *Planet. Space Sci.*, **32**, 1291–1300, 1984.
- Keskinen, M. J., R. N. Sudan, and R. L. Ferch, Temporal and spatial power spectrum studies of numerical simulations of type

- II gradient drift irregularities in the equatorial electrojet, *J. Geophys. Res.*, **84**, 1419–1430, 1979.
- Koehler, J. A., G. J. Sofko, D. Andre, M. Maguire, R. Osterried, M. McKibben, J. Mu, D. Danskin, and A. Ortlepp**, The SAPPHIRE auroral radar system, *Can. J. Phys.*, **73**, 211–226, 1995.
- Kustov, A. V., and M. V. Uspensky**, Altitude integration effects in the skewness of type 2 coherent echoes, *Annales Geophysicae*, **13**, 946–953, 1995.
- Kustov, A. V., J. A. Koehler, G. J. Sofko, D. Danskin, and M. McKibben**, Observations of 50-MHz type-II coherent echoes from within the polar cap, *Annales Geophysicae*, **12**, 765–774, 1994.
- Kustov, A. V., G. C. Hussey, J. A. Koehler, G. J. Sofko, and J. Mu**, Spectral width of type 2 coherent echoes at large magnetic aspect angles, *J. Geophys. Res.*, **100**, 5733–5742, 1995.
- Kustov, A. V., J. A. Koehler, G. J. Sofko, and D. Danskin**, SAPPHIRE-North radar experiment: observations of diffuse and discrete auroral coherent echoes, *J. Geophys. Res.*, **101**, 7973–7986, 1996.
- Kustov, A. V., J. A. Koehler, G. J. Sofko, D. Danskin, and A. Schiffler**, Relationship of the SAPPHIRE-North merged velocity and the plasma convection velocity derived from simultaneous SuperDARN radar measurements, *J. Geophys. Res.* **102**, 2495–2501, 1997.
- Nielsen, E., and K. Schlegel**, Coherent radar Doppler measurements and their relationship to the ionospheric electron drift velocity, *J. Geophys. Res.*, **90**, 3498–3504, 1985.
- Osterried, R. B.**, The SAPPHIRE data collection system and observations of radar aurora from the pre-SAPPHIRE system, M. Sc. Thesis, University of Saskatchewan, Saskatoon, Canada, 1993.
- Osterried, R., A. V. Kustov, G. J. Sofko, J. A. Koehler, and A. André**, On the spectral asymmetry of type II coherent echoes at large magnetic aspect angles, *J. Geophys. Res.*, **100**, 9707–9715, 1995.
- Sudan, R. N.**, Unified theory of type I and type II irregularities in the equatorial electrojet, *J. Geophys. Res.*, **88**, 4853–4860, 1983.
- Uspensky, M. V., and P. J. S. Williams**, The amplitude of auroral backscatter, 1, Model estimates of the dependence on electron density, *J. Atmos. Terr. Phys.*, **50**, 73–79, 1988.
- Uspensky, M. V., P. J. S. Williams, V. I. Romanov, V. G. Pivovarov, G. J. Sofko, and J. A. Koehler**, Auroral radar backscatter at off-perpendicular aspect angles due to enhanced ionospheric refraction, *J. Geophys. Res.*, **99**, 17,503–17,509, 1994.
- Yeoman, T. K., M. Lester, D. Orr and H. Luhr**, Ionospheric boundary conditions of hydromagnetic waves: the dependence on azimuthal wavenumber and a case study, *Planet. Space Sci.*, **38**, 1315–1325, 1990.